Journal of Renewable and Sustainable Energy

Reliability based optimal DG planning for a meshed distribution network

Cite as: J. Renewable Sustainable Energy **11**, 066301 (2019); https://doi.org/10.1063/1.5115207
Submitted: 15 June 2019 . Accepted: 16 October 2019 . Published Online: 05 November 2019

P. S. Meera, and S. Hemamalini

Journal of Renewable and Sustainable Energy ARTICLE scitation.org/journal/rse

Reliability based optimal DG planning for a meshed distribution network

Cite as: J. Renewable Sustainable Energy **11**, 066301 (2019); doi: 10.1063/1.5115207
Submitted: 15 June 2019 · Accepted: 16 October 2019 ·
Published Online: 5 November 2019

View Online Export Citation CrossMark

P. S. Meera and S. Hemamalini

AFFILIATIONS

School of Electrical Engineering, Vellore Institute of Technology, Chennai, India

ABSTRACT

Distributed generation (DG) sources are becoming more popular nowadays because of their technoeconomic and environmental benefits. These benefits are maximized only when the DG sources are properly planned and installed in the distribution networks. Several studies have been carried out in this field considering various objectives and constraints, for single as well as multiple DG placement and sizing. In this paper, an optimization methodology based on particle swarm optimization is used for the optimal planning of multiple DG sources in a meshed distribution network. The solution consists of the possible DG locations, DG capacities, and its operating power factor. The objectives considered are the improvement of reliability indices namely the system average interruption frequency index and system average interruption duration index, reduction of real power loss, and voltage profile improvement. Unlike other works, reliability evaluation is done considering many realistic constraints and it is used as one of the criteria for DG planning. Reliability indices are evaluated using the encoded Markov cut set algorithm. The real power loss and the voltage index are obtained by means of a simple load flow technique. The stochastic nature of the renewable DG output and the load are taken into account during the reliability evaluation along with islanding probability. The optimal planning of DG sources is done for bus 4 of the Roy billinton test system consisting of seven feeders, 102 nodes, and 106 components. Optimal planning for solar based DG sources is done considering three different load models namely residential, commercial, and mixed load.

I. INTRODUCTION

In recent years, there is a tremendous increase in the integration of distributed generation (DG) sources into the main grid. This increased penetration is attributed to the various advantages of having these sources located near the loads. In addition to the economic and environmental benefits, the major technical benefits of DG[1] are reduced losses, increased reliability, improved voltage profile, reactive power support to grid, and improved power quality and stability. The capacity of DG varies from few kilowatts (kW) to megawatts (MW)[2] and they are usually located in the distribution network. DGs can be either renewable based like photovoltaic, wind, tidal, etc. or conventional type like microturbines, fuel cells, oil based, etc. When DGs are introduced into the network, the power flow becomes bidirectional and this can cause many undesirable effects in the existing traditional distribution network which is designed to be a passive network. Renewable based DGs have intermittent power output characteristics and this can lead to decreased reliability and power quality unless properly planned. Hence, careful planning is needed for the installation and operation of these types of sources. Proper placement and sizing of DG sources are required to maximize the benefits of DG integration.

Most of the works in the literature focused on finding the optimal location and size for single or multiple DGs considering minimization of losses, improvement of voltage profile, cost benefit maximization, reliability improvement, short circuit mega-volt amperes (MVA), and voltage stability. The optimization approaches that have been applied[3] include both classical methods like linear programming and evolutionary algorithms like Particle Swarm Optimization (PSO), Genetic Algorithm (GA), Artificial Bee Colony, and nondominated sorting GA. Optimal siting and sizing of DG are done for a meshed network[4] considering losses, voltage profile, and short circuit MVA. Multiobjective PSO is used for DG integration,[5] considering maximization of DG owner's profit and minimization of Distribution Company's cost. The importance of optimal integration of DGs[6] in a distribution network and the various techniques used for obtaining the optimal solutions are discussed. An adaptive robust short-term planning of electrical distribution systems considering siting and sizing of renewable energy based DG units is done[7] using mixed integer liner programming. A new two-step optimization algorithm is proposed[8] for optimal placement of a wind turbine generator in a distribution network. The locations and power factors of the generators are obtained using lightning attachment procedure optimization in the first stage and then, the optimal capacities of the wind generators are determined analytically. A simulated annealing based method is proposed[9] for optimal integration of DG sources with a reliability criterion. Optimal siting and sizing of multiple DGs are obtained using the weighted sum method[10] and the problem is solved using GA and PSO. The objectives considered are the reduction of real and reactive power loss, improvement of voltage profile, stability, reliability, and sensitivity. The optimal planning of DG sources[11] is done without changing the traditional relay protection schemes. Different load models as well as the feeder failure rates[12] are also considered. A comprehensive review[13–15] about the various methodologies used, objectives, and constraints considered for the optimal siting and sizing of DG sources is presented.

Most of the optimal DG planning works done so far in the literature have considered the distribution network to be radial. For a meshed distribution network, the sectionalizing/tie switches are opened and the network is considered as radial during analysis. Only a few works have considered reliability during the DG planning process for a meshed network. Most of the authors who considered reliability as an objective function have evaluated the energy not supplied (ENS) index obtained from the power flow analysis or the system average interruption frequency index (SAIFI) and the system average interruption duration index (SAIDI) values obtained from the failure/repair rate available. The effects of DG failures or the DG islanding probability are not taken into account during reliability evaluation. In this paper, the above-mentioned drawbacks are addressed and the optimization for the siting and sizing of the multiple DGs in a meshed distribution network is done using particle swarm optimization. The objectives considered are maximization of reliability, minimization of real power loss, and improvement of voltage profile. While evaluating reliability, adequacy of the DG to supply the load during islanding, DG mechanical failure, starting/switching probability of the DG, and the distribution network failure are taken into account. The stochastic nature of the output of renewable energy based DG sources and the load are also taken into consideration. The DG planning solutions are obtained for solar energy based DGs for three types of load profiles namely residential, commercial, and mixed load. The proposed solution methodology is tested on bus 4 of the Roy billinton test system (RBTS) which has 7 feeders, 102 nodes including 38 load points, and 106 components. The tie lines are removed from the test system to consider it as a radial network and then, the simulations are repeated to obtain the DG planning solutions. This is performed to compare the DG planning solutions obtained for the meshed and radial network.

II. PROBLEM FORMULATION

The multiobjective function is formulated with the help of the weighted sum method. Four indices are evaluated namely, the system average interruption frequency index ($\mathrm{SAIFI_{DG}}$), system average interruption duration index ($\mathrm{SAIDI_{DG}}$), real power loss ($\mathrm{P_{lossDG}}$), and voltage index ($\mathrm{V_{indexDG}}$). Each index is divided by its corresponding base value for normalization. The weights can be fixed depending upon the importance of the objectives and the system behavior. The reliability indices evaluated are the expected values and they are obtained analytically by means of the encoded Markov cut set (EMCS) algorithm. The power loss and voltage index are obtained from load flow analysis.

A. Objective function

The objective function is to minimize the function, F, formulated as in (1)

$$Minimize\left\{\begin{array}{c} F = w_1 * \left(\dfrac{\mathrm{SAIFI}_{DG}}{\mathrm{SAIFI}_{NoDG}}\right) + w_2\left(\dfrac{\mathrm{SAIDI}_{DG}}{\mathrm{SAIDI}_{NoDG}}\right) \\ + w_3\left(\dfrac{P_{\mathrm{loss}_{DG}}}{P_{\mathrm{loss}_{NoDG}}}\right) + w_4\left(\dfrac{V_{\mathrm{index}_{DG}}}{V_{\mathrm{index}_{NoDG}}}\right) \end{array}\right\}, \tag{1}$$

$$\mathrm{w_1 + w_2 + w_3 + w_4 = 1}, \tag{2}$$

where F is the objective function; SAIFI and SAIDI are the reliability indices; and $\mathrm{P_{loss}}$ and $\mathrm{V_{index}}$ are the power loss and voltage indices. $\mathrm{w_1}$, $\mathrm{w_2}$, $\mathrm{w_3}$, and $\mathrm{w_4}$ are the weights associated with each index with the sum of the weights equal to one as given in (2). SAIFI and SAIDI are evaluated using (3) and (4)

$$SAIFI = \frac{\sum \lambda_i N_i}{\sum N_i}, \tag{3}$$

$$SAIDI = \frac{\sum U_i N_i}{\sum N_i}. \tag{4}$$

where λ_i is the failure rate, N_i is the number of customers at load point i, and U_i is the annual outage time of load point i.[16] Real power loss, $\mathrm{P_{loss}}$ and voltage index, $\mathrm{V_{index}}$ are given by (5) and (6).

$$P_{Loss} = \sum\nolimits_{m=1}^{N} \left(I_m^2 R_m\right), \tag{5}$$

$$V_{index} = \sum_{i=1}^{n} \Sigma(1 - V_\mathrm{i}), \tag{6}$$

where I_m is the current and R_m is the resistance of the branch m, N is the total number of branches in the system, V_i is the voltage of node i *and n is the total number of nodes*. The voltage index is calculated using (6) so as to minimize the voltage deviation of all nodes from the flat voltage profile.

B. Constraints

The objective function is minimized subjected to the following constraints given in (7)–(12).

(1) Power balance constraints

$$\mathrm{P_G = P_D + P_{Loss}}, \tag{7}$$

$$\mathrm{Q_G = Q_D + Q_{Loss}}, \tag{8}$$

where $\mathrm{P_G}$ and $\mathrm{Q_G}$ are the total real and reactive power generation, $\mathrm{P_D}$ and $\mathrm{Q_D}$ are the total real and reactive power demand, and $\mathrm{P_{Loss}}$ and $\mathrm{Q_{Loss}}$ are the total real and reactive power loss of the distribution network.

(2) Voltage limits

$$V_{\min} \le V_i \le V_{\max}, \tag{9}$$

where $\mathrm{V_{min}}$ and $\mathrm{V_{max}}$ are the minimum and maximum voltage of the $\mathrm{i^{th}}$ node.

(3) DG capacity limits

$$DG_{\min} \le DG_{cap} \le DG_{\max} \tag{10}$$

where $\mathrm{DG_{cap}}$ is the capacity of the installed DG and $\mathrm{DG_{min}}$ and $\mathrm{DG_{max}}$ are the minimum and maximum capacity of the installed DG source.

(4) DG node limits

$$Bus_i \leq DG_{node} \leq Bus_n \quad (11)$$

DG_{node} is the location for the DG installation; Bus_i and Bus_n are the first and last node, respectively, in the list of nodes available for DG installation.

(5) Operating power factor (PF) limits

$$PF_{\min} \leq PF_{DG} \leq PF_{\max} \quad (12)$$

where PF_{DG} is the operating power factor of the DG, PF_{min} is the minimum operating power factor, and PF_{max} is the maximum operating power factor of the DG.

The solar DG along with the voltage source inverter can function similar to a static synchronous compensator (STATCOM). STATCOM can regulate the voltage at its terminal by controlling the amount of reactive power injected into or absorbed from the grid. During day time, the inverter exchanges reactive power with the grid using the inverter capacity remaining after real power injection. It operates as a STATCOM with full inverter capacity in nighttime as well as during any time of the day to provide critical grid support.

The following four cases for DG output are analyzed.

(a) Type 1: Only real power is generated and there is no reactive power support to the grid. Power factor will be maintained at unity.
(b) Type 2: Real power is supplied and reactive power is absorbed. Operating power factor of the DG will be lagging.
(c) Type 3: Both real and reactive power is generated. Operating power factor of the DG will be leading.
(d) Type 4: Operating power of the DG can be either lagging or leading.

III. SOLUTION METHODOLOGY

The multiobjective optimal DG integration problem is solved with the help of particle swarm optimization along with EMCS and load flow algorithms. In each iteration of the PSO algorithm, the reliability indices are evaluated by means of the EMCS algorithm and the loss and voltage indices are obtained by performing the load flow analysis. Then, the fitness function is calculated from the obtained indices using the weighted sum method.

A. Particle swarm optimization

Particle swarm optimization, proposed by Kennedy and Eberhart, is an evolutionary algorithm inspired by social behavior of birds.[17] A set of particles are initialized randomly and then, they are made to fly through the search space in search of the global minimum. This is achieved by updating the velocity and position of the particles as in (13) and (14). PSO is almost similar to the genetic algorithm except that it does not have any evolutionary operators like crossover or mutation. PSO is used for single or multiple objective functions either as a maximization or minimization algorithm. It has a fewer number of operators and is easy to implement and the time taken to converge to the final solution is very less.

$$V_{i+1} = w * V_i + C_1 * rand * (localbest_i - X_i) + C_2 * rand * (globalbest_i - Xi), \quad (13)$$

$$X_{i+1} = X_i + V_{i+1}, \quad (14)$$

where V_{i+1} and V_i are the velocity, X_{i+1} and X_i are the position of the particle for the $(i+1)^{th}$ and i^{th} iteration, respectively, w is the inertia weight, and C_1 and C_2 are the positive constant coefficients.

B. Encoded Markov cut set (EMCS) algorithm

The EMCS algorithm is an analytical method for reliability evaluation[18] which uses both minimal cut set and Markov modeling to calculate the reliability. The method is algorithmic in nature and hence can be used for the reliability centric optimal planning of the distributed generation systems. The following reduction techniques are applied in order to simplify and thus bring down the number of system states. During reliability evaluation, only one load point will be considered at a time. The components which do not belong to any of the paths connecting the source and the load are removed from the network. The remaining components, if possible, are reduced with the help of series parallel combinations. The maximum number of simultaneous failures is also limited to three. These reduction techniques reduce the number of system states drastically. Prime number encoding for the components helps in creating a unique ID for each set of lines. Then, the concept of Petri Nets is used to identify the minimal tie sets. The remaining sets of lines are further classified into tie sets, cut sets, and minimal cut sets. The individual load point indices are evaluated first and then, the system reliability is evaluated based on the number of customers. After incorporating DG into the network, reliability is evaluated considering the DG mechanical failure rate, its adequacy to supply the load during islanding, and its starting/switching probability. The variation in the output of renewable energy based DG sources and the load are taken into account by developing the capacity probability table (CPT) and demand probability table (DPT). CPT and DPT are convolved to find out the adequacy rate of the DG to supply the load. This detail is used while developing the 10 state Markov model[19] for the system. Each component is represented by two states, namely UP and DOWN. The state transition matrix for the Markov model is developed and then solved with the help of Kolmogorov equations. The 10 state Markov model used for the distribution system reliability analysis is shown in Fig. 1.

C. Load flow analysis

The load flow method used in this paper is based on two matrices,[20] namely, the bus injection to branch current matrix (BIBC) and branch current to bus voltage matrix (BCBV). For meshed distribution networks, to account for the loops, new branches are added without altering the bus current injections. Load flow solution is obtained by solving (15)–(19)

$$\begin{bmatrix} B \\ B_{new} \end{bmatrix} = [BIBC] \begin{bmatrix} I \\ B_{new} \end{bmatrix}, \quad (15)$$

where B is the branch current of the radial network, B_{new} is the current corresponding to the new branch which has to be added to make the system meshed, and I is the bus current injection.

$$\begin{bmatrix} \Delta V \\ 0 \end{bmatrix} = [BCBV] \begin{bmatrix} B \\ B_{new} \end{bmatrix}, \quad (16)$$

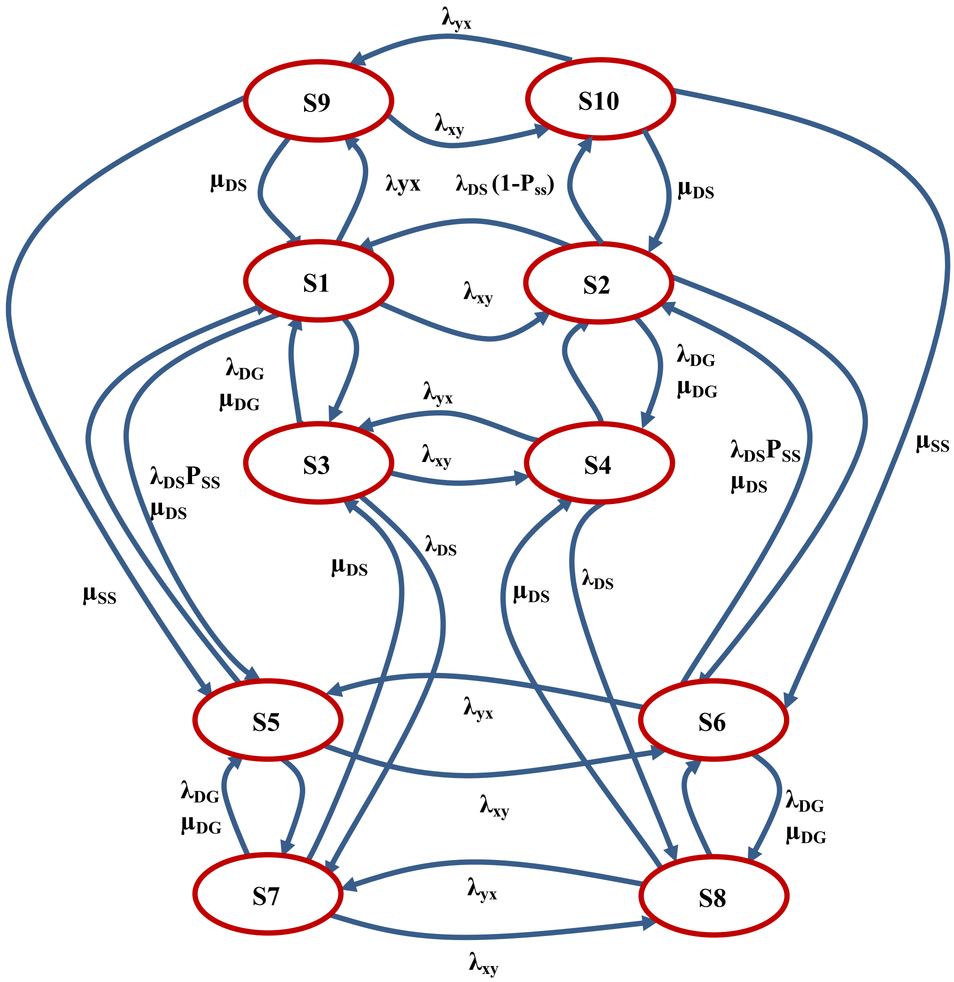

FIG. 1. Markov model for the distribution system.

$$\begin{bmatrix} \Delta V \\ 0 \end{bmatrix} = [BCBV][BIBC]\begin{bmatrix} I \\ B_{new} \end{bmatrix} = \begin{bmatrix} A & M^T \\ M & N \end{bmatrix}\begin{bmatrix} I \\ B_{new} \end{bmatrix}, \tag{17}$$

where ΔV is the difference in node voltages. After applying Kron's reduction, (17) simplifies to (18)

$$\Delta V = [A - M^T N^{-1} M][I] = [DLF][I]. \tag{18}$$

Since the DGs considered in this research are integrated into the grid by means of power electronics interface, a constant power factor model is used for modeling DGs. The equivalent current injections are calculated for the DGs[21] and then incorporated into the load flow technique. If the voltage at the node is V_{DG}, then the equivalent current injection, I_{DG}, is given by

$$I_{DG} = \left(\frac{P_{DG} + jQ_{DG}}{V_{DG}}\right)^*, \tag{19}$$

where P_{DG} and Q_{DG} are the real and reactive power output of the installed DG source, respectively.

IV. IMPLEMENTATION OF THE OPTIMIZATION ALGORITHM

The proposed optimization algorithm is implemented with the help of the following step by step procedure. The flow chart for the algorithm is given in Fig. 2.

(1) Input the line data, load data, reliability data, number of customers, annual renewable DG output data, and the connection matrix for the given meshed distribution network.
(2) Evaluate the two matrices, BIBC and BCBV and the bus current injections, I for the given system.
(3) Run the load flow for the test system without DGs and obtain the real power loss ($P_{lossNoDG}$) and the voltage deviation index ($V_{index\ NoDG}$) as per (5) and (6).
(4) Reduce the system states by applying various reduction techniques and limiting the maximum number of simultaneous failures to three.
(5) Using prime number encoding, generate the master list of all the system states and with the help of Petri Nets identify the minimal tie sets. Classify the remaining states into tie sets, cut sets, and minimal cut sets.
(6) With the help of Markov modeling and state transition matrix, obtain the load point reliability indices and then the system reliability indices, SAIFI and SAIDI for the system without DGs.

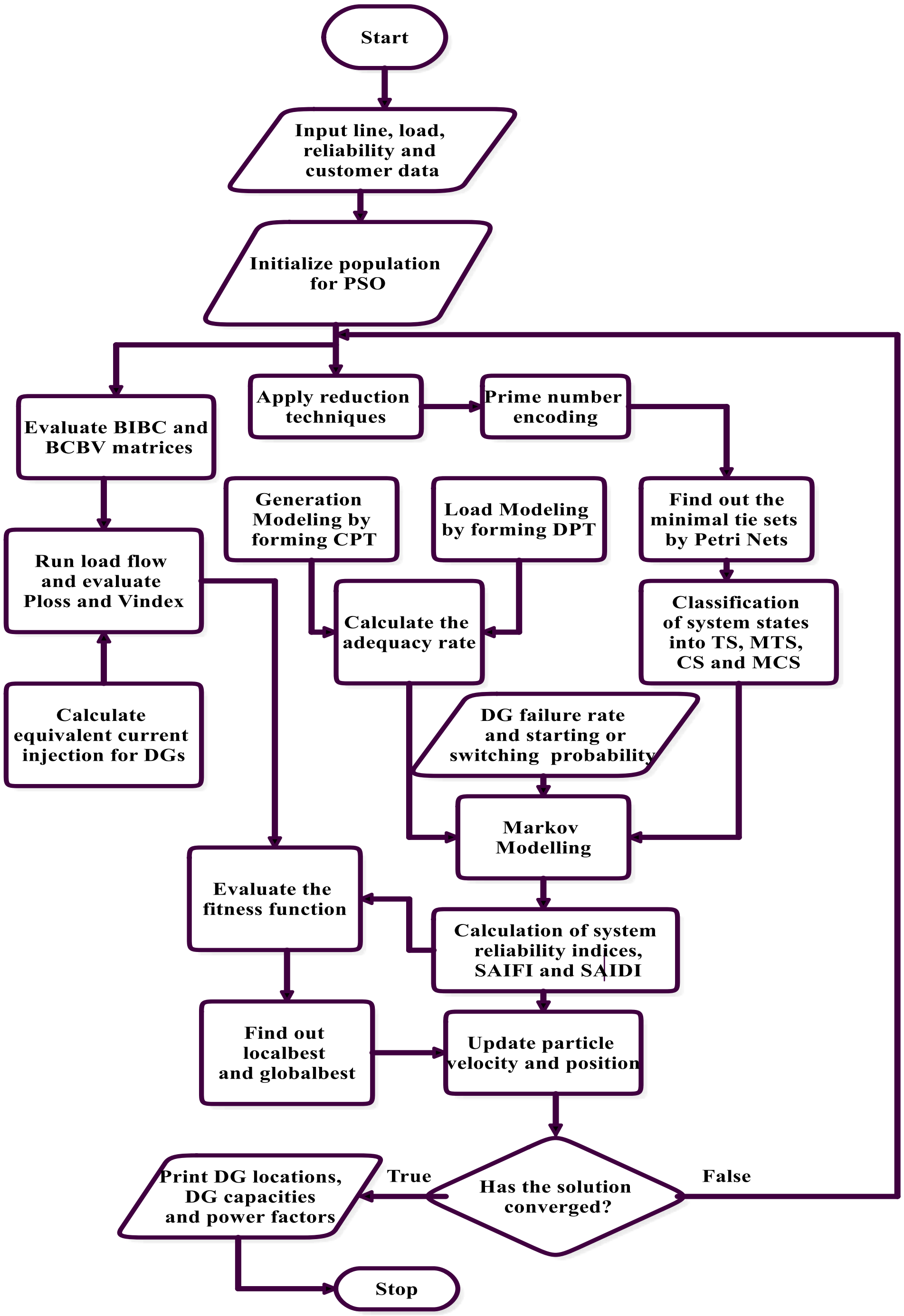

FIG. 2. Flow chart for the optimization algorithm.

(7) Initialize the population sets for PSO, namely $\{P_1, P_2, \ldots, P_n\}$, $\{N_1, N_2, \ldots, N_n\}$ and $\{PF_1, PF_2, \ldots, PF_n\}$ and its initial velocities, where "n" is the number of particles in a population, P_i is the real power output of the DG sources, N_i is the location for DG installation, and PF_i is the operating power factor of the DGs. Specify the possible DG location nodes, i.e., between Bus_i and Bus_n, the minimum (DG_{min}) and maximum capacity (DG_{max}) for the DGs and the range of operating power factor.

(8) Calculate the equivalent bus current injection for DG using (19) and then perform the load flow algorithm given by (15)–(18).

(9) Generate DPT and CPT. Convolve the two tables to obtain the adequacy rate.

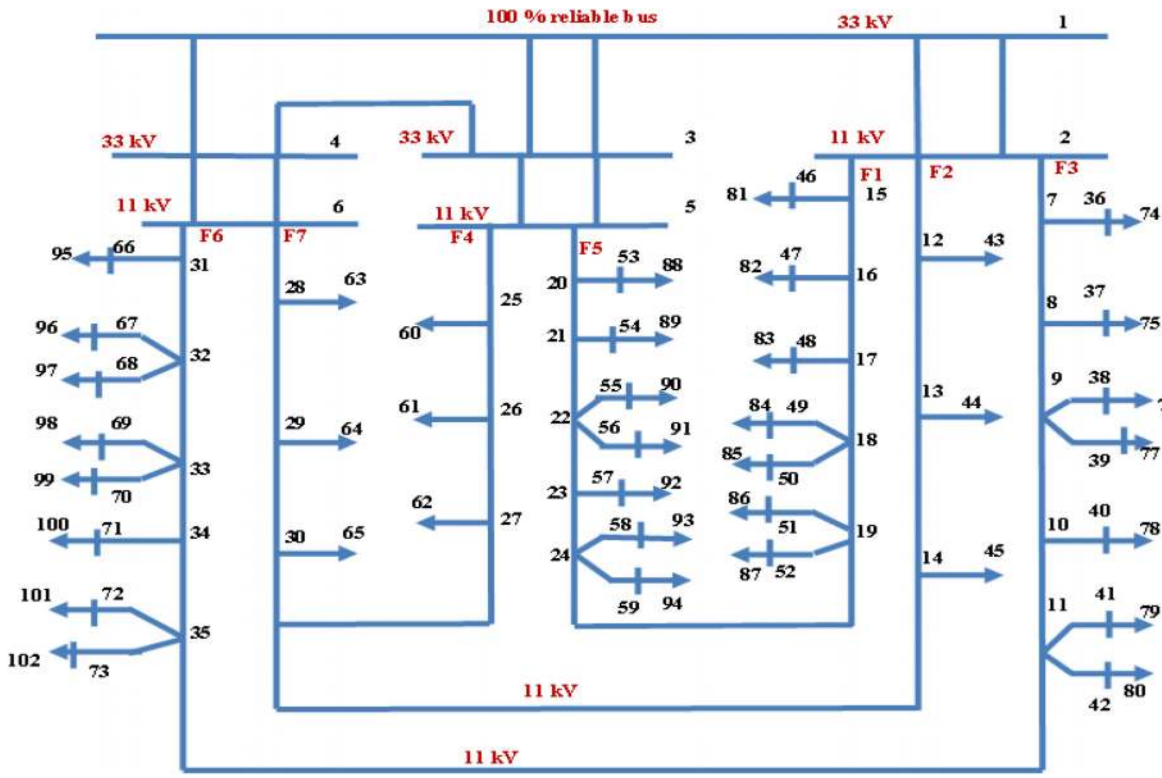

FIG. 3. Single line diagram for the RBTS Bus 4 distribution network.

(10) Markov modeling for the system is done with the DG failure rate and the starting/switching probability data.
(11) Calculate the reliability indices as per Eqs. (3) and (4).
(12) Evaluate the objective function in terms of all four indices by means of the weighted sum method using (1) and (2).
(13) Calculate the velocity and position of the new particles using (13) and (14).
(14) The set of particles of the each iteration is considered as the local best ($localbest_i$).
(15) Evaluate the fitness function for the updated set of particles by repeating the procedure from step 8 until step 12. Set the global best to be the particle set which gives the minimum value among all the particles and the local best to be the solution which gives the minimum for each set of particles.
(16) Repeat steps 14 and 15 until the maximum number of iterations is reached or when the solution has converged to the minimum value.

The final solution will be the DG capacities, DG locations, and the operating power factor depending upon the number of DGs to be installed.

V. RESULTS AND DISCUSSION

The multiobjective problem is solved using the PSO algorithm in MATLAB installed in a personal computer having Intel® Core™, 2.5 GHz, 8 GB RAM. The population size for the PSO algorithm is 100 and the positive constant coefficients C1 and C2 are 2 each. The test system considered is bus 4 of RBTS which is commonly used for reliability studies and it is a meshed system. It has 7 main 11 kV feeders namely F1-F7, 102 nodes, and 106 components[22] as shown in Fig. 3. The data required for reliability studies such as the failure and repair rate are available for all the components for the test system. They have a total of 38 load points and 4779 customers. The total real power load of the system is 40 MW. Some loads are connected at the secondary side of the 11/0.415 kV transformer, whereas few are directly connected to the 11 kV feeder. All the tie lines and switches are assumed to be 100% reliable. Only overhead lines are considered for the reliability analysis. It is assumed that the DGs are operated always in parallel with the grid supply. The DG failure rate is considered to be 2 failures per year for the solar DG. The repair time is assumed to be 48 h. The probability to start or switch DG is assumed to be 0.95 with a repair time of 12 h.[19] During islanding, it is assumed that the DG gets disconnected if it is not able to supply the load. It is assumed that during islanding, DG will be supplying the load if it is located in the

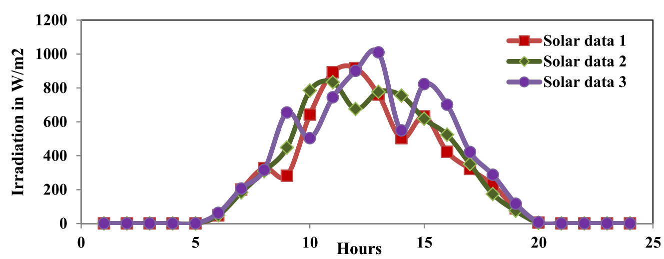

FIG. 4. Three different sets of annual irradiation data for solar based DG sources.

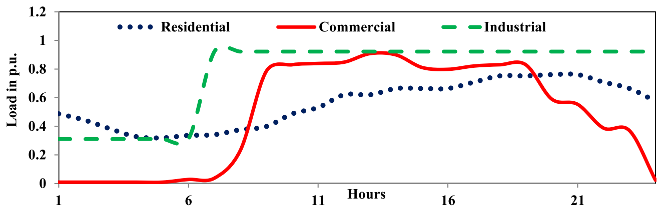

FIG. 5. Hourly data for the different load models.

same lateral having the load node. Three DGs are considered for the analysis along with three types of customer load patterns, namely residential, commercial, and mixed load. The test system is divided into three regions with feeders 1, 2, and 3 in region 1, feeders 4 and 5 in region 2, and feeder 6 and 7 in region 3. For solar DG, three regions are considered with three different annual irradiation data as shown in Fig. 4. The solar irradiation data are taken from the NREL database for three different sites in California, namely, San Francisco, San Jose, and Santa Rosa.[23] Figure 4 shows the solar irradiation data for 24 h for a partial cloudy day in the month of June. The per unit load is modeled[24] as per the following equation:

$$L(t) = P_w P_d P_h(t), \tag{20}$$

where P_w is the percentage of weekly load in terms of annual peak load, P_d is the percentage of daily load in terms of the weekly peak load, and P_h is the percentage of the hourly load in terms of the daily peak. The load models for different customers used in this research are shown in Fig. 5. For the base case, no DGs are integrated into the network. But four switched capacitor banks each of 1 MVar capacity are installed at nodes having minimum voltage namely 18, 19, 34, and 87. For this base case, the value of reliability index, SAIFI is obtained as 0.0616 and SAIDI as 3.2261. The real power loss and the voltage index for the same case with peak load are 0.2930 p. u. and 4.9707, respectively. During optimization, the value of the weights w_1, w_2, w_3, and w_4 is considered to be equal to 0.25 so as to give equal importance for all the objectives. The minimum and maximum limit for the power factor is set at 0.85 and 1.00, respectively. Voltage at each node should be maintained between 0.95 and 1.05 p. u. DGs are installed only at the 11 kV nodes and the capacity varies from 1 MW to 10 MW.

A. Case 1—Residential load

The optimal DG planning solutions are obtained for solar based DG sources and are given in Table I. In this case, when the load is residential in nature, the minimum fitness function value is obtained for type 3 solar based DG. The corresponding DG capacities are 3.21, 3.35, and 4.08 MW installed at nodes 49, 42, and 35, respectively. Their operating power factors are 0.86, 0.87, and 0.92. Figure 6 shows the hourly box plot of voltage for all the 102 nodes. Load variation for the first day in the month of January is considered for the plot. It is clear from the figure that all the node voltages are well within the voltage constraint. When type 3 solar DGs are placed at nodes 49, 42, and 35, the voltage index improves to 1.74. From Fig. 7, it can be concluded that the SAIFI index is improved by 6.5% when type 2 solar based DGs are installed at nodes 46, 16, and 49 having capacities 1.33, 5.27, and 2.09 MW. Their operating power factors are 0.91, 0.96, and 0.92, respectively. For the same solution set, the SAIDI index is improved by 6.8%. Real power loss is reduced by 74% for type 3 DGs as shown in Fig. 8. In practice, DGs can be operated at lagging or leading power factor and for this case, the fitness function is obtained as 0.7272.

B. Case 2—Commercial load

The optimal DG planning solutions for commercial load are given in Table II. The minimum fitness function value of 0.6543 is obtained for type 3 solar DGs. Figure 9 illustrates the hourly box plot of all node voltages when type 3 DGs are installed in the network. The variations in node voltages are much more when compared with the residential load. This can be attributed to the difference in the load pattern for commercial load when compared with the residential load.

TABLE I. Optimal DG planning solutions for residential load.

Nature of DG	DG node	DG size (MW)	DG PF	SAIFI	SAIDI	P_{loss} (p.u.)	V_{index} (p.u.)	Fitness function
Solar type 1	49	1.99	Unity	0.0588	3.0794	0.1020	3.3209	0.7313
	16	3.43	Unity					
	28	5.22	Unity					
Solar type 2	46	1.33	0.91 lagging	0.0576	3.0073	0.1269	3.7093	0.7616
	16	5.27	0.96 lagging					
	49	2.09	0.92 lagging					
Solar type 3	49	3.21	0.86 leading	0.0606	3.1463	0.0768	1.7419	0.6429
	42	3.35	0.87 leading					
	35	4.08	0.92 leading					
Solar type 4	49	5.60	0.96 leading	0.0578	3.012	0.1906	1.9195	0.7272
	16	4.86	0.98 lagging					
	17	6.27	0.86 leading					

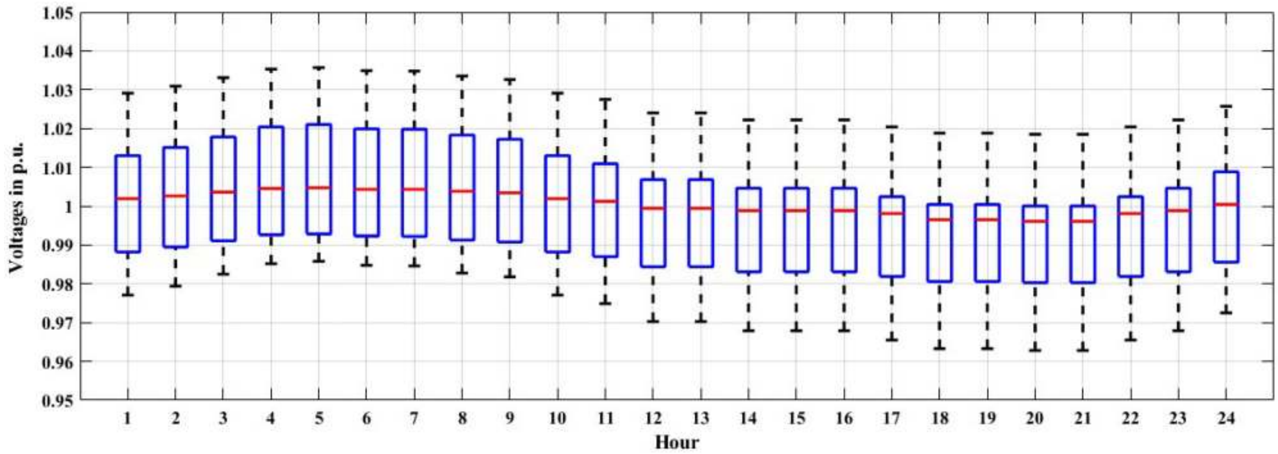

FIG. 6. Hourly box plot of voltage for a day-residential load.

The maximum node voltage deviation is obtained for solar, type 2 DGs and the corresponding voltage index is 3.7048. The best DG planning solution is obtained for type 3 solar DGs when installed at nodes 49, 35, and 42. From Fig. 10, it is clear that the maximum improvement in reliability indices is obtained for type 1 solar DG sources and the percentage improvement for SAIFI and SAIDI is 4.7% and 4.5%, respectively. Figure 11 depicts the percentage improvement for reduction in real power loss and voltage index for all types of DGs. Highest percentage improvement is obtained for type 3 DGs.

C. Case 3—Mixed load

Usually, the loads will not be purely residential or commercial in nature. In order to consider the realistic scenario which prevails in the distribution network, a mixed load scenario is also analyzed. In this case, the load comprises residential, industrial, and commercial loads. The DG planning solutions obtained are given in Table III.

The best solution is obtained for type 3 solar DGs when installed at nodes 16, 28, and 62. Figure 12 shows the hourly box plot of node voltages for the mixed load condition. The highest voltage index value of 3.8032 is obtained for type 2 solar DGs. The variation in the node voltages is highest for this case among all the obtained solutions.

Under the peak load condition, the minimum voltage value obtained for the base case is 0.8969 p. u. whereas it is improved to 0.9502 for residential and 0.9505 for commercial customers. The voltage index is best for type 3 solar DGs when load is residential in nature and the worst for type 2 solar DGs for the mixed load condition. Figure 13 compares the voltage profile plot of the best and the worst DG planning solutions obtained in terms of voltage index with the base case. It is clear from the plot that all the node voltages are within the limits of the voltage constraint.

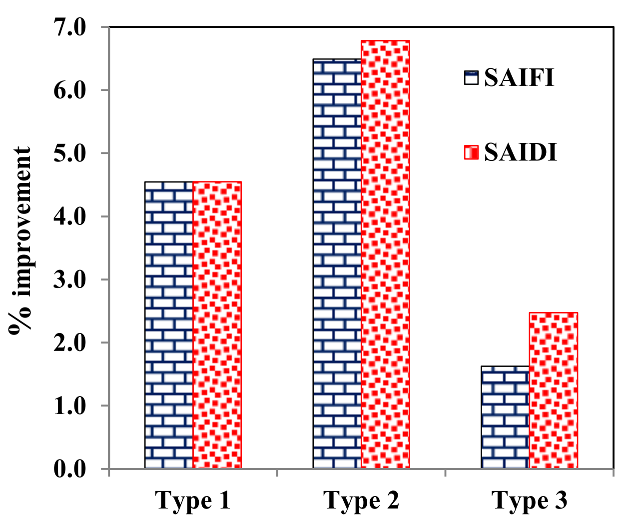

FIG. 7. Percentage improvement in reliability indices for residential load.

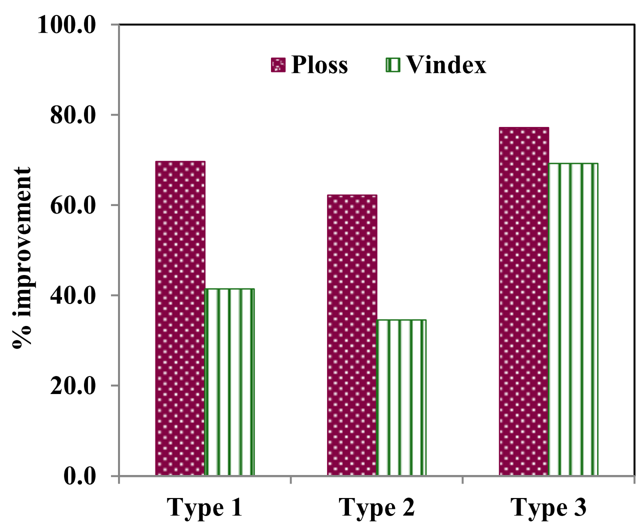

FIG. 8. Percentage improvement in real power loss and voltage deviation for residential load.

TABLE II. Optimal DG planning solutions for commercial load.

Nature of DG	DG node	DG size (MW)	DG PF	SAIFI	SAIDI	P_{loss} (p.u.)	V_{index} (p. u.)	Fitness function
Solar type 1	49	2.21	Unity	0.0587	3.0794	0.1025	3.3643	0.7335
	16	1.91	Unity					
	29	4.43	Unity					
Solar type 2	15	3.07	0.89 lagging	0.0590	3.0808	0.1201	3.7048	0.7670
	47	1.67	0.90 lagging					
	63	2.62	0.94 lagging					
Solar type 3	49	2.74	0.92 leading	0.0606	3.1461	0.0759	1.9847	0.6543
	35	4.43	0.94 leading					
	42	3.06	0.87 leading					
Solar type 4	48	5.76	0.90 lagging	0.0592	3.1293	0.1172	2.9547	0.7314
	49	5.30	0.87 leading					
	16	4.41	0.87 lagging					

The improvements in the real power loss and voltage deviation indices are higher compared to the reliability indices. The percentage improvement in the loss reduction can be attributed to the reduced distance between the source and the load. The percentage improvement in the reliability indices is limited, because many realistic factors are considered for reliability analysis and hence, the results obtained will be more pessimistic in nature. Also it is clear from the results that improvement in real power loss reduction or voltage profile does not guarantee an increase in reliability. For all the cases, solar type 3 DGs give the best performance. It can be concluded that the system performance improves if DG provides reactive power support. Type 3 DGs will supply reactive power in addition to real power which results in improvement of the grid power factor. Since the node voltages for the case without DG sources is not very high, more amount of reactive power needs to be supplied by the DGs for the improvement of the voltage profile. Hence, the DG power factor is not close to unity. Type 2 DGs can handle the overvoltage condition which occurs when the DG penetration increases. In this paper, only three DGs are installed simultaneously and all the loads are considered to be inductive in nature. Hence, type 3 DGs give the best fitness function value for all the cases.

Table IV shows the variation in DG locations and DG capacities with variation in weights of the objective function. For the comparison, type 1 solar DGs are considered. It is observed that when the weights vary, the capacity as well as the nodes for DG installation varies widely along with the fitness function value. The fitness function is minimum when the weights w_1, w_2, w_3, and w_4 are set at 0.1, 0.1, 0.1, and 0.7 and maximum when the values are 0.7, 0.1, 0.1, and 0.1. The time taken by the algorithm to converge to the optimal solution is around 1484.33 s. The PSO algorithm is repeated 20 times with 2000 iterations for each run. The convergence characteristic of the optimization algorithm is shown in Fig. 14.

Table V shows the DG planning solutions obtained for the RBTS BUS 4 radial network for residential load. The meshed system is

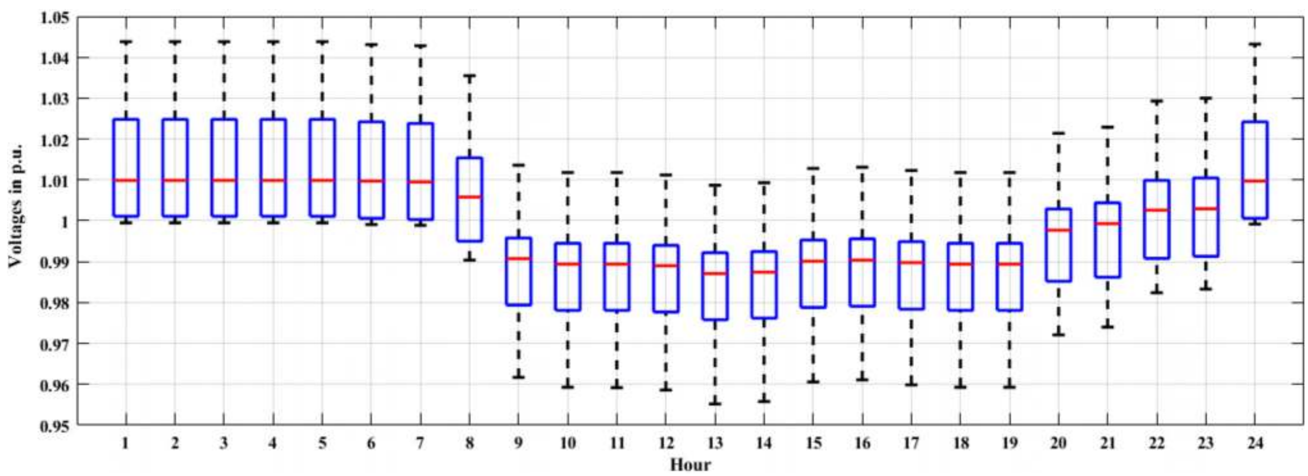

FIG. 9. Hourly box plot of voltage for a day-commercial load.

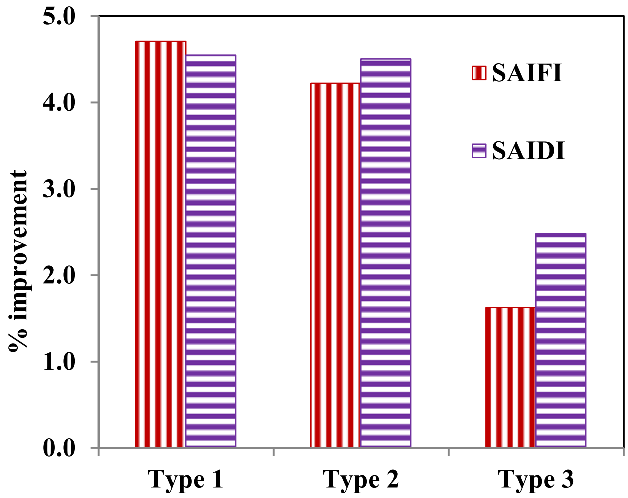

FIG. 10. Percentage improvement in reliability indices for commercial load.

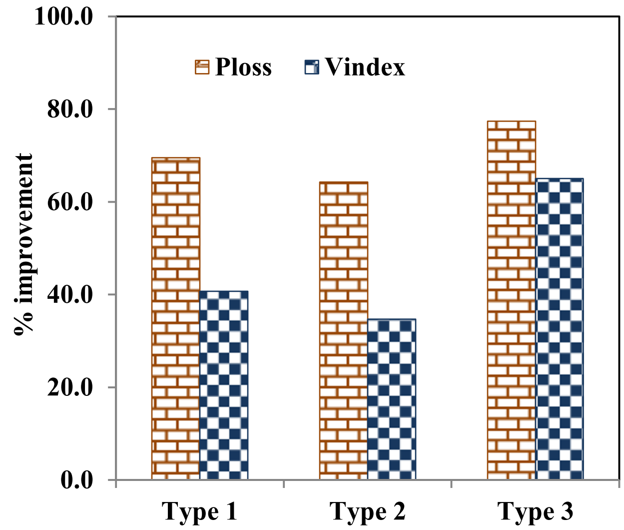

FIG. 11. Percentage improvement in real power loss and voltage deviation for commercial load.

converted into a radial system by removing the tie lines. The best solution is obtained for type 3 DGs. But when compared with the meshed network results of Table I, it is clear that the values of SAIFI, SAIDI, $P_{loss,}$ and V_{index} are very much higher for the radial network. The voltage profile improves by 61.3% for the meshed network with DG compared to the radial network. Upon integration of type 3 DGs into the system, the real power loss reduces by around 25.72%. The reliability of the meshed system is also higher compared to the radial network as multiple paths are available for connecting different sources and the load. SAIFI is improved by 68.8% and SAIDI is improved by around 13.38% for solar type 3 DGs.

VI. CONCLUSION

A novel PSO based DG planning methodology giving due importance to reliability along with power loss and voltage profile is proposed in this paper. The optimization is done for a 102 bus meshed distribution network connected to bus 4 of RBTS. Reliability is evaluated using an encoded Markov cut set algorithm considering many realistic parameters like DG failures, probability of successful starting and switching of the DG, and probability of islanding during failures. The stochastic nature of renewable DG output as well as the load is taken into consideration during the reliability analysis along with different types of renewable DG sources and customers.

Unlike other works, when all these factors are considered for DG planning, it gives the distribution network operator a clear picture about the various implications of placement of the renewable energy sources on the distribution network performance. The advantage of the proposed method is that the entire process including Markov modeling, finding the minimal cut sets, reduction of the system states and load flow can be written in an algorithmic manner and hence, the

TABLE III. Optimal DG planning solutions for mixed load.

Nature of DG	DG node	DG size (MW)	DG PF	SAIFI	SAIDI	P_{loss} (p.u.)	V_{index} (p.u.)	Fitness function
Solar type 1	49	3.38	Unity	0.0603	3.1494	0.0881	3.0685	0.7183
	28	7.42	Unity					
	24	3.79	Unity					
Solar type 2	46	2.63	0.92 lagging	0.0576	3.0073	0.1207	3.8032	0.7611
	16	2.37	0.87 lagging					
	49	1.21	0.93 lagging					
Solar type 3	16	5.81	0.90 leading	0.0602	3.1529	0.0776	2.7287	0.6921
	28	7.18	0.86 leading					
	62	3.90	0.88 leading					
Solar type 4	48	4.36	0.83 leading	0.0589	3.1276	0.1327	2.9883	0.7449
	49	9.93	0.94 lagging					
	47	1.57	0.90 lagging					

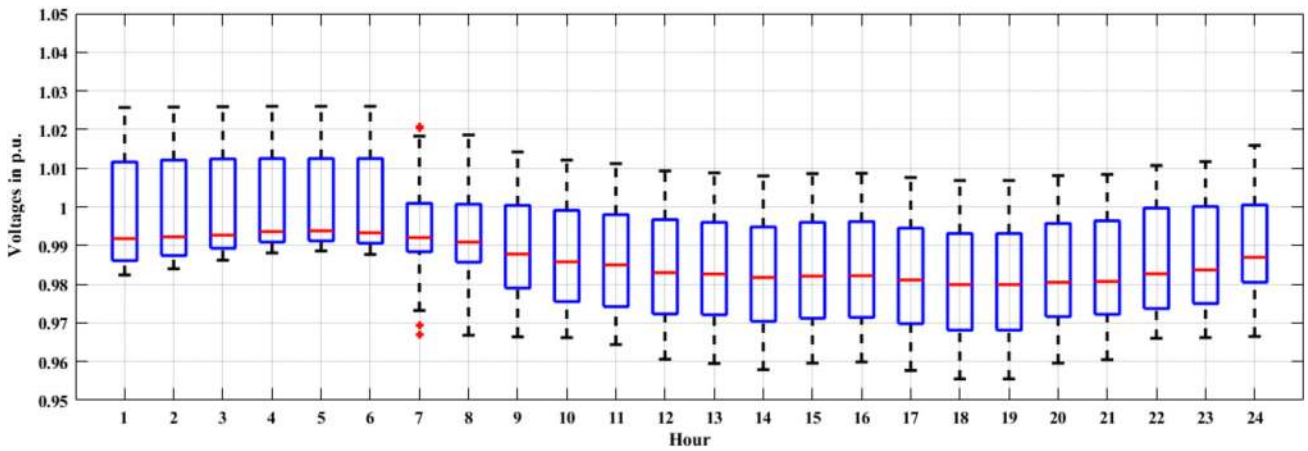

FIG. 12. Hourly box plot of voltage for a day-mixed load.

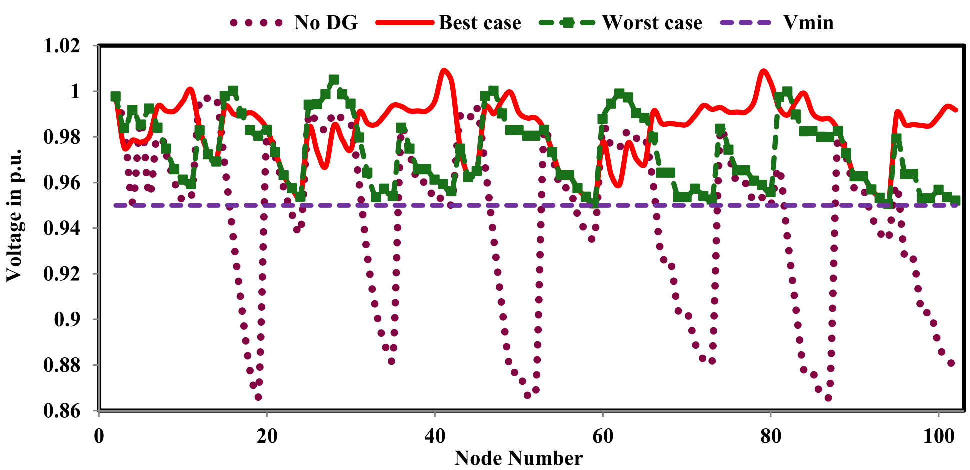

FIG. 13. Voltage profile plot for peak load condition.

method can be extended for larger networks and there is no bias in the calculations.

Among the DG planning solutions obtained for all the cases, there is a maximum improvement of about 7% each in the SAIFI and SAIDI indices. Real power loss reduces by 74% and the voltage profile index improves by 67% when compared with the case without DG sources. It can be concluded that the inherent uncertainty in the generation of renewable energy based DG sources will not degrade the network performance but improves, if they are properly planned and installed in the distribution network. Real power loss reduction or voltage profile improvement does not guarantee an increase in the reliability indices. Hence, reliability is given due importance along with other technical constraints for DG planning in this paper. The distribution

TABLE IV. Variation in DG planning solutions for solar, type 1 DGs with variation in weights.

w_1, w_2, w_3, w_4	DG locations	DG capacities	Fitness function
0.7, 0.1, 0.1, 0.1	15, 49, 16	6.52, 1.00, 3.51	0.7851
0.1, 0.7, 0.1, 0.1	49, 46, 16	1.02, 4.55, 2.02	0.7823
0.1, 0.1, 0.7, 0.1	11, 61, 33	3.08, 4.89, 5.88	0.3592
0.1, 0.1, 0.1, 0.7	49, 42, 35	2.07, 3.30, 4.66	0.2273
0.2, 0.3, 0.4, 0.1	11, 62, 35	4.72, 2.69, 5.87	0.5926
0.3, 0.4, 0.1, 0.2	17, 49, 15	1.61, 2.07, 1.02	0.6909

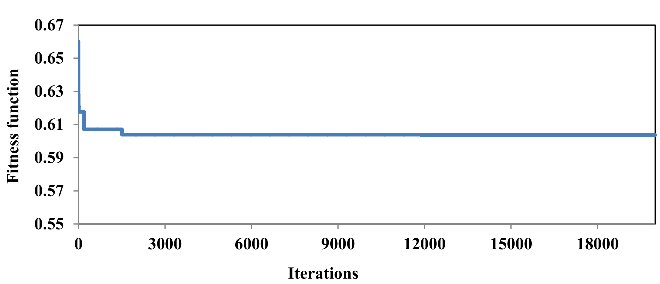

FIG. 14. Convergence characteristics of the optimization algorithm.

TABLE V. Optimal DG planning solutions for the radial network.

DG Type	DG node	DG size (MW)	DG PF	SAIFI	SAIDI	P_{loss} (p.u.)	V_{index} (p.u.)	Fitness function
Solar type 1	49	2.25	Unity	0.1851	3.6209	0.1153	4.8195	0.9231
	18	4.9	Unity					
	34	9.88	Unity					
Solar type 2	48	1.86	0.90 lagging	0.1903	3.6338	0.1264	4.9006	0.9526
	15	1.34	0.92 lagging					
	33	9.97	0.98 lagging					
Solar type 3	18	9.78	0.82 leading	0.1940	3.6322	0.1034	4.4993	0.8987
	33	6.04	0.86 leading					
	34	4.91	0.95 leading					
Solar type 4	15	3.43	0.90 lagging	0.1843	3.5874	0.1189	4.8364	0.9265
	49	5.76	0.97 leading					
	34	8.76	0.92 lagging					

network performance can be further enhanced if the installed DGs are able to provide reactive power support to the grid in addition to real power. Moreover, when the distribution network is operated as a meshed system, there is an improvement in reliability, power loss reduction, and voltage profile when compared with the radial topology.

REFERENCES

[1] T. Ackermann, G. Andersson, and L. Soder, "Distributed generation: A definition," Electr. Power Syst. Res. **57**, 195 (2001).
[2] W. El-Khattam and M. M. A. Salama, "Distributed generation technologies, definitions and benefits," Electr. Power Syst. Res. **71**, 119 (2004).
[3] T. Adefarati and R. C. Bansal, "Integration of renewable distributed generators into the distribution system: A review," IET Renewable Power Gener. **10**(7), 873 (2016).
[4] M. M. Elnashar, R. El Shatshat, and M. M. A. Salam, "Optimum siting and sizing of a large distributed generator in a mesh connected system," Electr. Power Syst. Res. **80**, 690 (2010).
[5] A. Ameli, S. Bahrami, F. Khazaeli, and M.-R. Haghifam, "A multiobjective particle swarm optimization for sizing and placement of DGs from DG owner's and distribution company's Viewpoints," IEEE Trans. Power Delivery **29**(4), 1831 (2014).
[6] A. Colmenar-Santos, C. Reino-Rio, D. Borge-Diez, and E. Collado-Fernández, "Distributed generation: A review of factors that can contribute most to achieve a scenario of DG units embedded in the new distribution networks," Renewable Sustainable Energy Rev. **59**, 1130 (2016).
[7] O. D. Melgar-Dominguez, M. Pourakbari-Kasmaei, and J. R. S. Mantovani, "Adaptive robust short–term planning of electrical distribution systems considering siting and sizing of renewable energy based DG units," IEEE Trans. Sustainable Energy **10**(4), 158 (2019).
[8] A. Foroughi Nematollahi, A. Rahiminejad, B. Vahidi, H. Askarian, and A. Safaei1, "A new evolutionary-analytical two-step optimization method for optimal wind turbine allocation considering maximum capacity," J. Renewable Sustainable Energy **10**, 043312 (2018).
[9] J. Mitra, M. R. Vallem, and C. Singh, "Optimal deployment of distributed generation using a reliability criterion," IEEE Trans. Ind. Appl. **52**(3), 1989 (2016).
[10] A. K. Bohre, G. Agnihotri, and M. Dubey, "Optimal sizing and sitting of DG with load models using soft computing techniques in practical distribution system," IET Gener., Transm. Distrib. **10**(11), 2606 (2016).
[11] H. Zhan, C. Wang, Y. Wang *et al.*, "Relay protection coordination integrated optimal placement and sizing of distributed generation sources in distribution networks," IEEE Trans. Smart Grid **7**(1), 55 (2016).
[12] M. Rahmani-andebili, "Distributed generation placement planning modeling feeder's failure rate and customer's load type," IEEE Trans. Ind. Electron. **63**(3), 1598 (2016).
[13] P. Prakash and D. K. Khatod, "Optimal sizing and siting techniques for distributed generation in distribution systems: A review," Renewable Sustainable Energy Rev. **57**, 111 (2016).
[14] A. Ehsan and Q. Yang, "Optimal integration and planning of renewable distributed generation in the power distribution networks: A review of analytical techniques," Appl. Energy **210**, 44 (2018).
[15] A. Rezaee Jordehi, "Allocation of distributed generation units in electric power systems: A review," Renewable Sustainable Energy Rev. **56**, 893 (2016).
[16] R. Billinton and R. N. Allan, *Reliability Evaluation of Power Systems* (Plenum, New York, 1996).
[17] J. Kennedy and R. C. Eberhart, "Particle swarm optimization," in Proceedings of the 1995 IEEE International Conference on Neural Networks, Perth, Australia, 1942 (1995).
[18] M. Al-Muhaini and G. T. Heydt, "A novel method for evaluating future power distributed system reliability," IEEE Trans. Power Syst. **28**(3), 3018 (2013).
[19] M. Al-Muhaini and G. T. Heydt, "Evaluating future power distributed system reliability including distributed generation," IEEE Trans. Power Delivery **28**(4), 2264 (2013).
[20] J.-H. Teng, "A direct approach for distribution system load flow solutions," IEEE Trans. Power Delivery **18**(3), 882 (2003).
[21] J.-H. Teng, "Modelling distributed generations in three-phase distribution load flow," IET Gener., Transm. Distrib. **2**(3), 330 (2008).
[22] R. N. Allan, R. Billington, I. Sjarief, L. Goel *et al.*, "A reliability test system for educational purposes—Basic distribution system data and results," IEEE Trans. Power Syst. **6**(2), 813 (1991).
[23] National Renewable Energy Laboratory (NREL), https://rredc.nrel.gov/solar/old_data/nsrdb/1991-2010/ for National Solar Radiation Data Base (NSRDB), 1991–2010.
[24] A. Jonnavithula, "Composite system reliability evaluation using sequential Monte Carlo simulation," Ph.D. dissertation (Department of Electrical Engineering, Saskatoon, SK, Canada, 1997).